J|A|C|S
ARTICLES
Published on Web 09/09/2006

A Modular Strategy for Tailoring Fluorescent Biosensors from Ribonucleopeptide Complexes

Masaki Hagihara,[†] Masatora Fukuda,[†] Tetsuya Hasegawa,[†] and Takashi Morii*[,†,‡]

Contribution from the Institute of Advanced Energy, Kyoto University, and SORST, JST, Uji, Kyoto 611-0011, Japan

Received June 6, 2006; E-mail: morii@iae.kyoto-u.ac.jp

Abstract: Fluorescent biosensors that facilitate reagentless sensitive detection of small molecules are crucial tools in the areas of therapeutics and diagnostics. However, construction of fluorescent biosensors with desired characteristics, that is, detection wavelengths and concentration ranges for ligand detection, from macromolecular receptors is not a straightforward task. An ATP-binding ribonucleopeptide (RNP) receptor was converted to a fluorescent ATP sensor without chemically modifying the nucleotide in the ATP-binding RNA. The RNA subunit of the ATP-binding RNP and a peptide modified with a pyrenyl group formed a stable fluorescent RNP complex that showed an increase in the fluorescence intensity upon binding to ATP. The strategy to convert the ATP-binding RNP receptor to a fluorescent ATP sensor was applied to generate fluorescent ATP-binding RNP libraries by using a pool of RNA subunits obtained from the in vitro selection of ATP-binding RNPs and a series of fluorophore-modified peptide subunits. Simple screening of the fluorescent RNP library based on the fluorescence emission intensity changes in the absence and presence of the ligand afforded fluorescent ATP or GTP sensors with emission wavelengths varying from 390 to 670 nm. Screening of the fluorescence emission intensity changes in the presence of increasing concentrations of ATP allowed titration analysis of the fluorescent RNP library, which provided ATP sensors responding at wide concentration ranges of ATP. The combinatorial strategy using the modular RNP receptor reported here enables tailoring of a fluorescent sensor for a specific ligand without knowledge of detailed structural information for the macromolecular receptor.

Introduction

Biosensors that directly transduce binding events into optical signals are useful tools in the areas of therapeutics and diagnostics.[1,2] Macromolecular receptors, such as proteins[3−10] and nucleic acids,[11−28] are chemically modified with reporter groups to transduce ligand binding into measurable optical signals. However, construction of fluorescent biosensors responding at desirable wavelengths and expedient ligand concentration ranges is not a straightforward task. The first step to construct a fluorescent biosensor requires an effort to find a macromolecular receptor with appropriate affinity and specificity to the target, which is not always available. The second step converts the macromolecular receptor to a fluorescent sensor commonly by chemical modification of the receptor with a fluorophore with suitable optical characteristics. Because the

[†] Kyoto University.
[‡] SORST.

(1) Zhang, J.; Campbell, R. E.; Ting, A. Y.; Tsien, R. Y. *Nat. Rev. Mol. Cell Biol.* **2002**, *3*, 906−918.
(2) Weiss, S. *Science* **1999**, *283*, 1676−1683.
(3) Pollack, S. J.; Nakayama, G. R.; Schultz, P. G. *Science* **1988**, *242*, 1038−1040.
(4) Renard, M.; Belkadi, L.; Hugo, N.; England, P.; Altschuh, D.; Bedouelle, H. *J. Mol. Biol.* **2002**, *318*, 429−442.
(5) Gilardi, G.; Zhou, L. Q.; Hibbert, L.; Cass, A. E. *Anal. Chem.* **1994**, *66*, 3840−3847.
(6) de Lorimier, R. M.; Smith, J. J.; Dwyer, M. A.; Looger, L. L.; Sali, K. M.; Paavola, C. D.; Rizk, S. S.; Sadigov, S.; Conrad, D. W.; Loew, L.; Hellinga, H. W. *Protein Sci.* **2002**, *11*, 2655−2675.
(7) Marvin, J. S.; Corcoran, E. E.; Hattangadi, N. A.; Zhang, J. V.; Gere, S. A.; Hellinga, H. W. *Proc. Natl. Acad. Sci. U.S.A.* **1997**, *94*, 4366−4371.
(8) Hamachi, I.; Nagase, T.; Shinkai, S. *J. Am. Chem. Soc.* **2000**, *122*, 12065−12066.
(9) Benson, D. E.; Conrad, D. W.; de Lorimier, R. M.; Trammell, S. A.; Hellinga, H. W. *Science* **2001**, *293*, 1641−1644.
(10) Morii, T.; Sugimoto, K.; Makino, K.; Otsuka, M.; Imoto, K.; Mori, Y. *J. Am. Chem. Soc.* **2002**, *124*, 1138−1139.
(11) Jayasena, S. D. *Clin. Chem.* **1999**, *45*, 1628−1650.
(12) Llano-Sotelo, B.; Chow, C. S. *Bioorg. Med. Chem. Lett.* **1999**, *9*, 213−216.
(13) Jhaveri, S.; Rajendran, M.; Ellington, A. D. *Nat. Biotechnol.* **2000**, *18*, 1293−1297.
(14) Stojanovic, M. N.; de Prada, P.; Landry, D. W. *J. Am. Chem. Soc.* **2000**, *122*, 11547−11548.
(15) Jhaveri, S. D.; Kirby, R.; Conrad, R.; Maglott, E. J.; Bowser, M.; Kennedy, R. T.; Glick, G.; Ellington, A. D. *J. Am. Chem. Soc.* **2000**, *122*, 2469−2473.
(16) Stojanovic, M. N.; de Prada, P.; Landry, D. W. *J. Am. Chem. Soc.* **2001**, *123*, 4928−4931.
(17) Fang, X. H.; Cao, Z. H.; Beck, T.; Tan, W. *Anal. Chem.* **2001**, *73*, 5752−5257.
(18) Stojanovic, M. N.; Landry, D. W. *J. Am. Chem. Soc.* **2002**, *124*, 9678−9679.
(19) Nutiu, R.; Li, Y. *J. Am. Chem. Soc.* **2003**, *125*, 4771−4778.
(20) Stojanovic, M. N.; Green, E. G.; Semova, S.; Nikic, D. B.; Landry, D. W. *J. Am. Chem. Soc.* **2003**, *125*, 6085−6089.
(21) Stojanovic, M. N.; Kolpashchikov, D. M. *J. Am. Chem. Soc.* **2004**, *126*, 9266−9270.
(22) Yamana, K.; Ohtani, Y.; Nakano, H.; Saito, I. *Bioorg. Med. Chem. Lett.* **2003**, *13*, 3429−3431.
(23) Ho, H. A.; Leclerc, M. *J. Am. Chem. Soc.* **2004**, *126*, 1384−1387.
(24) Kirby, R.; Cho, E. J.; Gehrke, B.; Bayer, T.; Park, Y. S.; Neikirk, D. P.; McDevitt, J. T.; Ellington, A. D. *Anal. Chem.* **2004**, *76*, 4066−4075.
(25) Savran, C. A.; Knudsen, S. M.; Ellington, A. D.; Manalis, S. R. *Anal. Chem.* **2004**, *76*, 3194−3198.
(26) Jiang, Y. X.; Fang, X. H.; Bai, C. L. *Anal. Chem.* **2004**, *76*, 5230−5235.
(27) Nutiu, R.; Li, Y. *Angew. Chem., Int. Ed.* **2005**, *44*, 1061−1065.
(28) Merino, E. J.; Weeks, K. M. *J. Am. Chem. Soc.* **2006**, *127*, 12766−12767.

10.1021/ja063965c CCC: $33.50

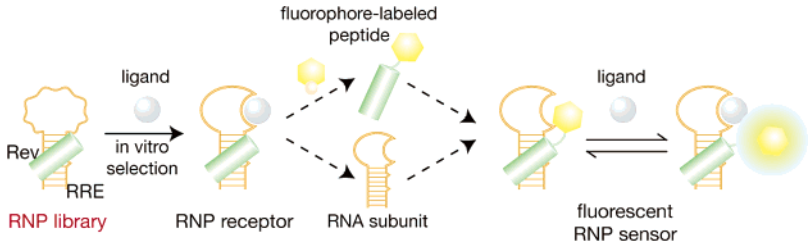

Figure 1. Scheme illustrating a direct conversion of a ribonucleopeptide (RNP) receptor to a fluorescent RNP sensor. A complex of the Rev peptide and RRE RNA[33] was used as a framework for the RNP receptor[30,31] and RNP sensor.

direct coupling between the ligand binding and the optical signaling events of fluorescent biosensors usually relies on the ligand binding-induced conformational change unique to each macromolecular receptor,[3−27] the fluorophore-labeled receptor is not always guaranteed to execute the expected optical signals. The chemical modification of the receptors to fluorescent sensors involves the following difficulties to overcome: (i) prediction of an appropriate position for the fluorophore modification and choice of a suitable fluorophore to exert desired emission properties of biosensors are challenging even with detailed structural information, and (ii) mutations or chemical modifications of biomolecular receptors often cause a loss of binding activity or stability of the parent receptor. Many mutants of the receptor are constructed and modified with a series of fluorophores, and then resulting fluorophore-labeled receptors have to be evaluated for the fluorescence responses to obtain macromolecular-based sensors with desired sensing properties.

The availability of receptors with appropriate affinity and specificity to the target has been expanded by in vitro selection[29] of RNA or DNA aptamers for targets ranging from small molecules to proteins or even cell membranes.[30] RNA or DNA aptamers have been utilized as macromolecular receptors to construct fluorescent aptamer sensors (sensing aptamers). Most fluorescent aptamer sensors have been chemically modified to incorporate fluorophore-labeled nucleotides into the aptamers,[11,12,14−20,22−26,28] which could cause the difficulties mentioned above.

We report here a new strategy that enables isolation of fluorescent ribonucleopeptide (RNP) sensors with a variety of binding and signal-transducing characteristics, that is, high signal-to-noise ratios, detection wavelengths, and concentration ranges for the ligand detection. The modular structure of RNP is ideal for construction of a fluorescent sensor without introducing a fluorophore-labeled nucleotide to the RNA aptamer (Figure 1). Adenosine 5′-triphosphate (ATP)-binding RNP receptors were obtained by in vitro selection of a library of stable RNP complexes[31,32] that consist of HIV Rev-peptide and its target RNA sequence RRE.[33] The RNA subunit of RNP was utilized to construct a ligand-binding cavity by in vitro selection, while further functionalization of the Rev peptide subunit was possible. An RNA subunit of the ATP-binding RNP and a Rev peptide modified with a pyrenyl group formed a stable fluorescent RNP complex that showed an increase in the fluorescence intensity upon binding to ATP. The above strategy to convert the ATP-binding RNP receptor to a fluorescent ATP sensor was applied to generate fluorescent ATP-binding RNP libraries. Combination of a pool of RNA subunits obtained from the in vitro selection of ATP-binding RNPs and a fluorophore-modified peptide subunit afforded the fluorescent RNP library, from which RNP sensors with expedient optical and binding properties were screened in a convenient manner. Changing the fluorophore of the peptide subunits generated fluorescent ATP-binding RNP libraries with various detection wavelengths, from which desired wavelength sensors were identified. The strategy consisting of a selection followed by a screen would potentiate generation of an array of fluorescent sensors for analytes with a variety of detection wavelengths and concentration ranges.

Results and Discussion

Conversion of an ATP-Binding RNP Receptor to a Fluorescent ATP Sensor. We first tested whether simple replacement of the Rev peptide of an ATP-binding RNP receptor with a fluorophore-labeled Rev peptide could afford a fluorescent ATP sensor (Figure 1). The ATP-binding RNP was obtained by in vitro selection as previously reported.[31,32] The size of random nucleotides within the RNA subunit was increased to 30 nucleotides (RRE30N) from the previously reported 20 nucleotides[31] to accomplish greater divergences in the RNA sequences of ATP-binding RNP at the first in vitro selection (Figure 2A).

The RNP receptors obtained by the in vitro selection against the ATP-agarose resin were tested for the ATP-binding characteristics. An RNP complex A23/Rev with a consensus 5′-GUAGUGG-UGUG-3′ sequence (Figure 2A) bound ATP with a dissociation constant (K_D) of 21.0 μM (Figure 2B) and discriminated ATP over other ribonucleotides GTP, CTP, and UTP efficiently (Figure 2C). Another RNP complex A28/Rev not sharing the consensus sequence in the RNA subunit (Figure 2A) also bound ATP efficiently with a K_D of 15.2 μM (Figure S1).

The A23/Rev RNP receptor was converted to a fluorescent ATP sensor by complexation of pyrene-labeled Rev (Pyr-Rev) and A23 RNA. This process was essentially the same as that described for the chemical modification of the macromolecular receptor by a fluorophore. In the present case, the N-terminal of the Rev peptide in the RNP receptor was chemically modified with a pyrene group. Fluorescence responses of RNP A23/Pyr-Rev were evaluated in the absence or presence of ATP. Addition of ATP resulted in a 2-fold increase of the fluorescence intensity of A23/Pyr-Rev (Figure 3A). A significant change in the fluorescence intensity of A23/Pyr-Rev was elicited only with ATP, not with other NTPs, indicating that the specificity of A23/Pyr-Rev to ATP is parallel to that of the parent A23/Rev receptor (Figure 3B). Titration of the changes in fluorescence intensities

(29) Ellington, A. D.; Szostak, J. W. *Nature* **1990**, *346*, 818−822.
(30) Wilson, D. S.; Szostak, J. W. *Annu. Rev. Biochem.* **1999**, *68*, 611−647.
(31) Morii, T.; Hagihara, M.; Sato, S.; Makino, K. *J. Am. Chem. Soc.* **2002**, *124*, 4617−4622.
(32) Sato, S.; Fukuda, M.; Hagihara, M.; Tanabe, Y.; Ohkubo, K.; Morii, T. *J. Am. Chem. Soc.* **2005**, *127*, 30−31.
(33) Battiste, J. L.; Mao, H.; Rao, N. S.; Tan, R.; Muhandiram, D. R.; Kay, L. E.; Frankel, A. D.; Williamson, J. R. *Science* **1996**, *273*, 1547−1551.

(A)

	RRE	Ligand Binding Region			RRE
A01	GGUCUGGGCGCA CCUUC	GUAGUGG	UGUUGUG	UGUG GUUGUUG	UGACGGUACAGGCC
A09	---------- CUGGUGU	GUAGUGG	GCUGUG	UGUG AUGCCG	----------
A14	---------- UACUGC	GUAGUGG	UUGGUG	UGUG GCGGUUU	----------
A15	---------- GCAGU	GUAGUGG	UUUGCG	UGUG AUUGCUUA	----------
A17	---------- UUAGAU	GUAGUGG	GUAGUG	UGUG UUUUCUG	----------
A21	---------- UUUGC	GUAGUGG	UUUUUGUG	UGUG GCUGUA	----------
A23	---------- UUAGAC	GUAGUGG	UUUUGUG	UGUG GUCUGC	----------
A24	---------- UGAUUGC	GUAGUGG	UUUGUG	UGUG GUUGUC	----------
A25	---------- UGCUG	GUAGUGG	GUAUGUG	UGUG CGGCAUU	----------
A26	---------- UUCCG	GUAGUGG	UUGUGUG	UGUG CGGUUUU	----------
A30	---------- UAUACC	GUAGUGG	UUUGUG	UGUG GGUUGG	----------
A31	---------- CAGAUU	GUAGUGG	CUUUUUGUG	UGUG AAUC	----------
A32	---------- UUGUAU	GUAGUGG	AUAUGUG	UGUG AUGCCG	----------
A33	---------- GUUUGCUGUUGCCGU	GUAGUGG	UUUG	UGUG	----------
A34	---------- U	GUAGUGG	UGCC	UGUG AUGGCUGUGUGUGA	----------
A35	---------- UCUUCU	GUAGUGG	UUUGCG	UGUG AGUUGUG	----------
A02	---------- UUGCAU	GUUGUGG	GUAUGUG	UGUG AUGUAU	----------
A08	---------- UUUUCAUGGCC	CUUGUGG	GAAGGAU	UGUG A	----------
A16	---------- UUGGCAC	GAAGUGG	UUUG	UGUG UGGUGUUU	----------
A36	----------	GUGGUGG	UUCG	UGUG GGUGCGCUGGUUUGU	----------
A29	----------	GUGG	UUGGUGGUC	UGUC GGGACGUGCUUGC	----------
A04	---------- AGGGCUUGGUGUGCCGAUUUCGGGGCAUU				----------
A28	---------- AGGGCUUGGUGUGCCGAUUUCGGGGCAUUU				----------
A05	---------- UUUCUCAGGUUUGUACUGUGCGUUGUCCAU				----------
A11	---------- UAGGGAUGUUGUGCGCACUUUGUGUCUCUU				----------
A07	---------- GAUGCUUGCCGUUUGUCAUGGUGUGGAGAG				----------
A22	---------- CUGUUUUGGCUUUACCGUUGUGGAACCCGU				----------
A06	---------- GUGUGGGUGGAAAGUAACCUGGCGUUUUUGUG				----------
A18	---------- AUUGGUCUUGUCUCGAUUUGGCGCUUCGCG				----------

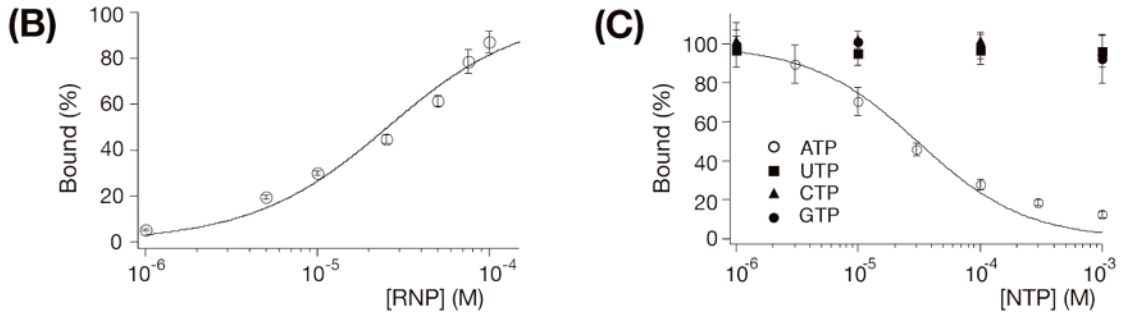

Figure 2. (A) Nucleotide sequences of the N30 ligand-binding region in the RNA subunit selected against ATP revealed possible consensus nucleotide sequences (shown in blue). RRE denotes the Rev-binding RNA sequence. (B) A saturation curve for the binding of A23/Rev (○) to immobilized ATP. A binding buffer (40 μL) containing 10 mM Tris-HCl (pH 7.6), 100 mM NaCl, 10 mM $MgCl_2$, 0.005% Tween20, ATP-agarose resin (9.2 μM), indicated amount of ^{32}P-labeled A23 RNA, and the Rev peptide complex was added to 0.2-μm spin filter column and allowed to equilibrate for 30 min. The binding mixtures were centrifuged for 1 min and immediately washed with 200 μL of binding buffer. Specifically bound RNA was eluted from matrix with 100 μL of elution buffer (5 mM ATP in binding buffer), followed by an additional wash (two times) with 100 μL of elution buffer. These eluates were combined and quantitated by Cherenkov counting in a scintillation counter. The fraction of A23/Rev specifically eluted as a function of immobilized ATP concentration was plotted and fitted as described previously.[31] (C) Competition binding assays of the ATP complex of the RNP receptor A23/Rev with ATP, UTP, CTP, or GTP indicate a selective ATP binding of A23/Rev. Binding reactions were performed in the presence of 1 M A23/Rev, a 20 μL volume of ATP-agarose resin, and 1 μM to 1 mM of ATP (○), UTP (■), CTP (▲), or GTP (●).

of A23/Pyr-Rev by ATP gave a K_D value of 19.5 μM for the A23/Pyr-Rev−ATP complex, which was in good agreement with the K_D value for the complex of parent A23/Rev and ATP (Figure 3B). In a similar manner, complexation of A28 RNA with Pyr-Rev afforded a fluorescent ATP sensor A28/Pyr-Rev (Figure 3C) with an affinity (K_D = 6.6 μM) comparable to the parent A28/Rev RNP receptor (K_D = 18.1 μM). The results indicate that reconstitution of the ATP-binding RNP receptor with a fluorophore-labeled Rev peptide simply and effectively converts ATP receptors into fluorescent ATP sensors without diminishing the affinity and selectivity of the parent ATP receptors.

Construction of Fluorescent RNP Libraries and Screening of Fluorescent RNP Sensors. In vitro selection of the ATP-binding RNP receptors generated a series of RNA sequences varying in the location of the consensus sequence within the randomized nucleotide region, affording a library of RNA subunits (Figure 2A). Each RNA subunit forms a ligand-binding pocket that has a unique geometry to the N-terminal of the Rev peptide and a defined affinity to the ligand in the RNP complex. Combination of the RNA subunit library and a fluorophore-labeled Rev peptide generates a library of fluorescent RNP receptors with a range of affinities and emission properties (Figure 4). Such a fluorescent RNP library would be ideal for

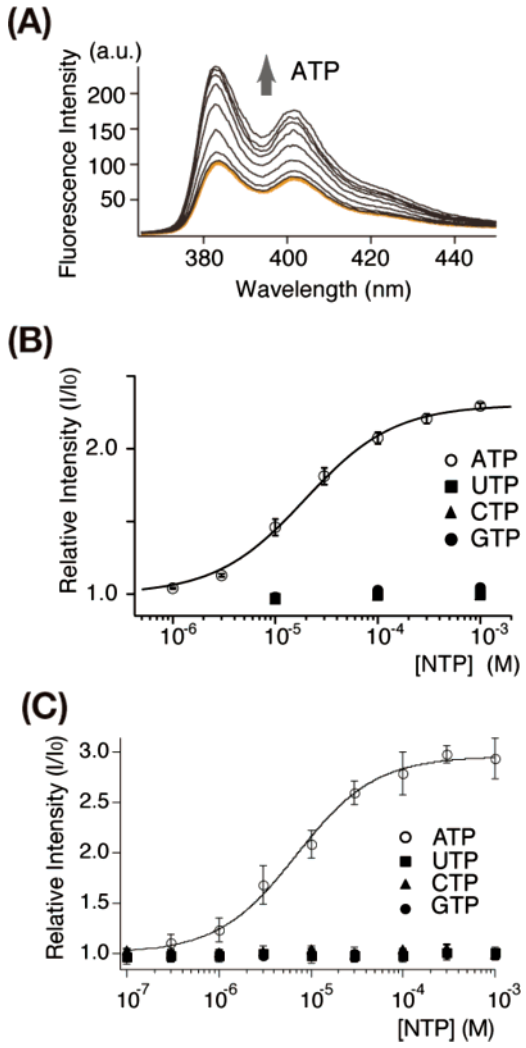

Figure 3. (A) Direct titration of a fluorescent RNP complex (0.1 μM) of the A23 RNA subunit and a Rev peptide modified with pyrene at the amino terminal (Pyr-Rev) with ATP (1, 3, 10, 30, 100, 300, 1000, and 3000 μM) shows an increase in fluorescence intensity of A23/Pyr-Rev. A spectrum in the absence of ATP is shown in red. (B) A saturation curve for the fluorescence emission intensity of A23/Pyr-Rev to ATP (○), UTP (■), CTP (▲), or GTP (●) indicates A23/Pyr-Rev responds selectively to the addition of ATP. (C) A saturation curve for the fluorescence emission intensity of A28/Pyr-Rev to ATP (○), UTP (■), CTP (▲), or GTP (●) indicates A28/Pyr-Rev responds selectively to the addition of ATP.

obtaining a fluorescent sensor tailor-made for a given target. Previous approaches, such as in vitro selection of fluorescently labeled aptamers[13] and the rational modular design of aptamer sensors,[21] could also be applicable to construct such sensor libraries.

The feasibility of the screening scheme of fluorescent RNP sensors (Figure 4) was demonstrated by using libraries of fluorescent RNP receptors constructed from the 29 different RRE30N RNAs obtained from the selection of ATP-binding RNP (Figure 2A) and Rev peptides modified with different fluorophores, 7-methoxycoumarin-3-carboxylic acid (7mC-Rev), 4-fluoro-7-nitrobenz-2-oxa-1,3-diazole (NBD-Rev), and Cy5 mono NHS ester (Cy5-Rev), at the N-terminal.

Each 7-methoxycoumarin-3-carboxylic acid-labeled Rev (7mC-Rev) and RNA complex was placed individually on a multi-well plate and was evaluated by the change of fluorescence intensities in the absence or presence of ATP (1 mM) by using a microplate reader. Figure 5A shows a scanned image of a multi-well plate assay of a fluorescent ATP-binding RNP library constructed from the RNA subunits of the ATP-binding RNP (Figure 2A) and 7mC-Rev. In most of the cases, the fluorescence emission of 7mC-Rev was quenched upon formation of RNP complexes as compared to that of 7mC-Rev alone (the lane marked "no RNA"). As typically shown in lanes 14, 23, 32, 34, 35, 02, 28, 07, and 06, the fluorescence emission increased in the intensity upon addition of ATP, indicating that these fluorescent RNPs could serve as ATP sensors.

The fluorescence intensities in the absence and presence of ATP were evaluated in a similar manner for fluorescent RNP libraries obtained by combination of the RNA subunits of the ATP-binding RNP and Pyr-Rev, NBD-Rev, and Cy5-Rev. Relative ratios of fluorescence intensity (I/I_0) in the absence (I_0) and the presence (I) of ATP for fluorescent RNPs with 7mC-Rev, Pyr-Rev, NBD-Rev, and Cy5-Rev monitored at 390, 390, 535, and 670 nm, respectively, were summarized in Figure 5B. The I/I_0 ratio of each sensor varied from 0.8 to 6. Considerable numbers of fluorescent ATP sensors responded with the I/I_0 ratio over 2 in all of the cases of fluorophores. The fluorescent RNP library with Cy5-Rev provided several ATP sensors with an emission at long wavelength (670 nm) and with I/I_0 ratios of over 2 (Figure 5B, panel d). Together, the above simple approach efficiently provided fluorescent ATP sensors emitting from 390 to 670 nm with excitation wavelengths ranging from 340 to 650 nm.

The degree to which the fluorescence intensity changed upon binding to ATP varied with each fluorescent RNP. A26 and

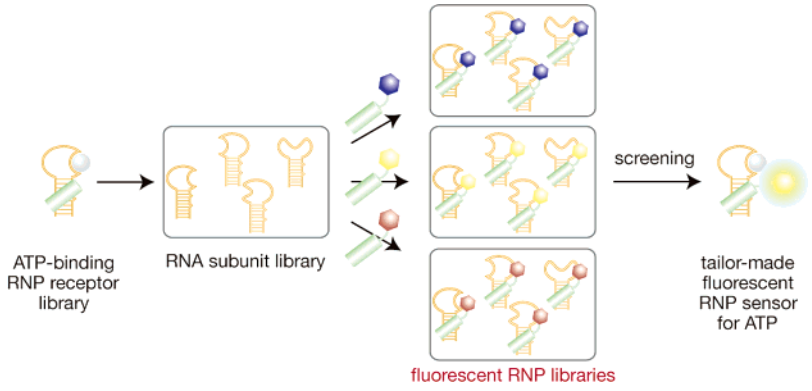

Figure 4. Scheme illustrating a screening strategy of a tailor-made RNP fluorescent sensor. Combination of the RNA subunit library of the RNP receptor and several fluorophore-labeled Rev peptide subunits generates combinatorial fluorescent RNP receptor libraries, from which RNP sensors with desired optical and/or binding properties are screened.

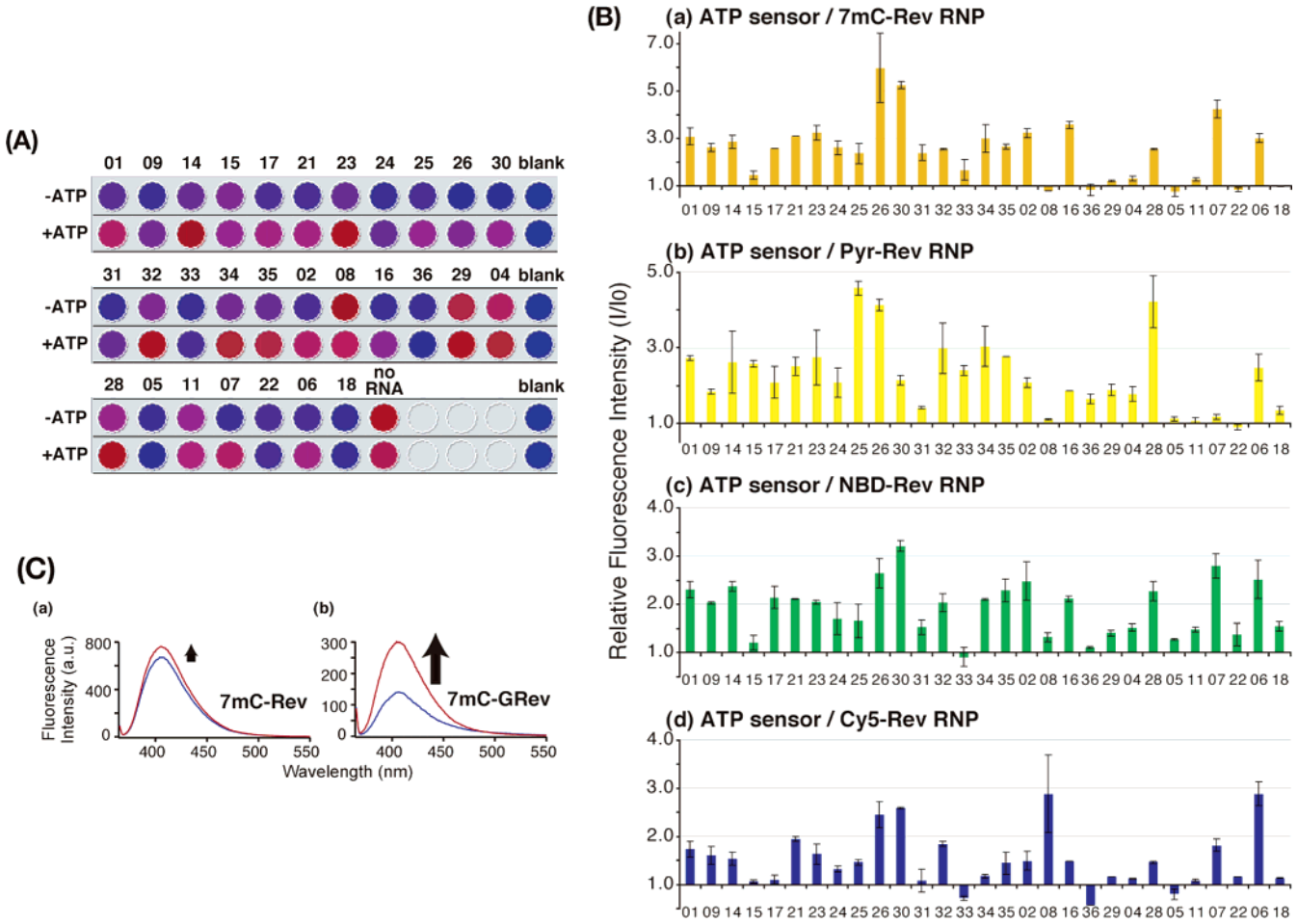

Figure 5. (A) A scanned image showing the microplate assay for the combinatorial screening of the fluorescent RNP library. Fluorescence intensities of 7mC-Rev derived RNPs (1 μM) were evaluated in the absence or presence of 1 mM of ATP with excitation at 355 nm and emission at 390 nm with intensities being weak in blue color and strong in red. The numerical designations of the fluorescent RNP complexes are in the same order as the RNA sequences presented in Figure 2A. (B) Relative fluorescence intensity changes (I/I_0) of RNPs upon ATP binding are shown in the bar graphs for (a) 7mC-Rev RNP, (b) Pyr-Rev RNP, (c) NBD-Rev RNP, and (d) Cy5-Rev RNP. (C) Modification of the linker of 7mC-Rev with an insertion of Gly residue (7mC-GRev) caused the changes in fluorescence intensity of RNP upon additions of ATP. Fluorescence emission spectra in the absence (blue) or presence (red) of 1 mM ATP are shown for (a) A08/7mC-Rev and (b) A08/7mC-GRev.

A30 RNAs afforded ATP sensors with high I/I_0 ratios both with 7mC-Rev and with NBD-Rev (Figure 5B, panels a and c). In contrast, even when the sensors were constructed from the same RNP receptor, the I/I_0 ratios varied with the fluorophore. A25/Pyr-Rev recorded the highest I/I_0 value of 4.5 within the Pyr-Rev sensors (Figure 5B, panel b), while A25/7mC-Rev showed a moderate I/I_0 ratio of 2.5 within the 7mC-Rev sensors (Figure 5B, panel a). These results confirmed the difficulty in predicting the efficiency of optical response of the fluorescence sensor and demonstrate the advantage of the above strategy to obtain usable fluorescence sensors. In the case of RNP sensors, the fluorophore at the N-terminal of Rev does not necessarily locate in the ligand-binding pocket composed by the RNA subunit to exhibit large fluorescence intensity changes upon ligand binding. The binding of ATP to the RNP sensor will cause conformational changes of the RNA subunit that can substantially alter the fluorescence intensity of the fluorophore.

Increasing the Size of the Fluorescent RNP Library. Expanding the size of the fluorescent RNP library facilitates an efficient screening of sensors with desired optical and/or binding activities. Fluorophores are often sensitive to a subtle microenvironmental change, which could be achieved by changing a tethering position of the fluorophore, or by introducing linkers with various length between the amino-terminal of Rev and the fluorophore. Such modifications expand the initial size of the fluorescent RNP library. To test this, a Rev derivative peptide with an additional Gly residue at the amino-terminal (GRev) was modified with 7-methoxycoumarin-3-carboxylic acid (7mC-GRev). The 7mC-GRev-derived RNP library revealed a pattern of I/I_0 ratios (Figure S3) different from that of the 7mC-Rev-derived RNP library (Figure 5B, a). Although the I/I_0 ratios of fluorescent RNPs were mostly decreased in the 7mC-GRev-derived RNP library, A08/7mC-GRev and A36/7mC-GRev showed improved I/I_0 ratios. As shown in Figure 5C, the observed I/I_0 ratio of A08/7mC-GRev was higher ($I/I_0 = 2.1$) than that of the original A08/7mC-Rev ($I/I_0 = 1.1$). Even using the same fluorophore, the I/I_0 ratio of fluorescent sensor was affected by a subtle change in the attaching position of the fluorophore on the peptide. Thus, derivatizing the fluorophore-attaching position of the Rev peptide also increased a diversity of the fluorescent RNP pool.

Screening of ATP Sensors Responding within Desired Concentration Ranges of ATP. The above simple screening scheme based on the relative changes in emission intensities of fluorescent RNPs with or without the ligand ATP (I/I_0) is quite useful for the screening of RNP sensors with desired emission

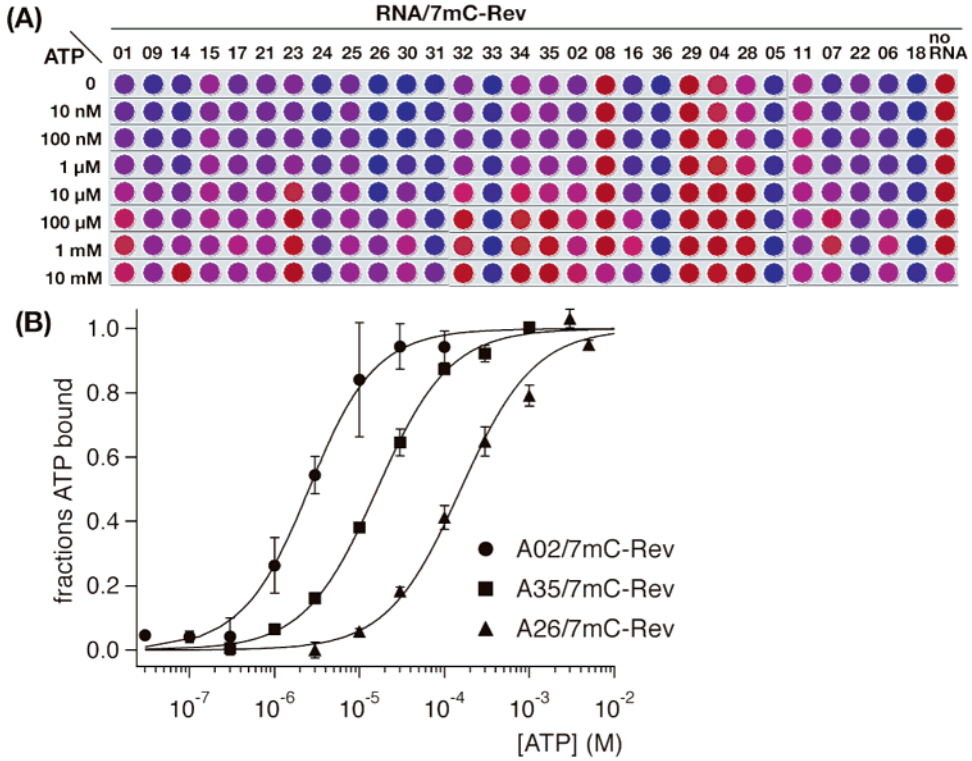

Figure 6. (A) Results of the microplate assay for the combinatorial screening of fluorescent RNP library with 7mC-Rev in the presence of 10 nM to 10 mM ATP visualize a concentration range of ATP for each fluorescent RNP to respond to effectively. The fluorescence intensities are weak in blue color and strong in red. (B) Saturation curves of 7mC-Rev RNPs A02/7mC-Rev (●), A35/7mC-Rev (■), and A26/7mC-Rev (▲) in the presence of 10 nM to 10 mM ATP were determined by titrations of fluorescence intensity changes.

wavelength and with high I/I_0 ratio. On the other hand, screening of the fluorescence emission intensities in the presence of increasing concentrations of ATP (10 nM to 10 mM) allowed titration analysis of the fluorescent RNP library, which enabled screening of ATP sensors responding within certain concentration ranges of ATP (Figure 6A). Evaluation of the fluorescence emission pattern versus the added ATP concentration instantly pointed to a concentration range at which each fluorescent RNP responds. For example, saturation midpoints of three sensors, A02/7mC-Rev, A35/7mC-Rev, and A26/7mC-Rev, were spaced at approximately 1 order of magnitude intervals (Figure 6B), with K_D values being 2.2, 15.7, and 156 μM, respectively. A fourth sensor, A31/7mC-Rev, began to show fluorescence response at the ATP concentration of 1−10 mM (Figure 6A). Simultaneous application of these four sensors covers ATP concentration ranges from $\sim 10^{-7}$ to $\sim 10^{-2}$ M.

Sensing Multiple Ligands at Different Wavelengths. The adaptability of in vitro selection to a panel of ligands[29,30] is fully applicable to the RNP-based selection scheme. RNP receptors for GTP were isolated from the pool of RNP by the in vitro selection method described for the selection of ATP-binding RNP.[31] Nucleotide sequences of the RNA subunit of GTP-binding RNPs revealed consensus 5′-GCGG-3′ and 5′-UGUC-UAC-3′ sequences (Figure 7A).

As with the case for the ATP-binding RNP, combination of the RNA subunit pool of the GTP-binding RNP and several fluorophore-labeled Rev peptide subunits gave combinatorial fluorescent RNP receptor libraries. The fluorescence intensities in the absence and presence of GTP were evaluated in a similar manner for fluorescent RNP libraries obtained by combination of the RNA subunits of the ATP-binding RNP and the fluorophore-labeled Rev peptides. A variety of fluorescent GTP sensors with I/I_0 ratios of over 2 were obtained from the fluorescent RNP libraries derived from the RNA subunit of GTP-binding RNP and 7mC-Rev, Pyr-Rev, or NBD-Rev (Figure 7B). In the case of the 7mC-Rev-derived GTP sensor library, G23/7mC-Rev, G26/7mC-Rev, G05/7mC-Rev, and G14/7mC-Rev had high I/I_0 ratios of over 4. As observed for the screen using the ATP sensor libraries, the observed I/I_0 ratios of GTP sensors depended on the nature of fluorophore even using the same RNA subunit. The I/I_0 ratio of G05/7mC-Rev, for example, reached almost 6 (Figure 7B, panel a), whereas that of G05/Pyr-Rev was measured to be 1 (Figure 7B, panel b).

These fluorescent GTP-binding RNPs showed distinct selectivity to GTP over other NTPs (Figure S3). With ATP and GTP sensors emitting at different wavelengths, concentrations of ATP and GTP in the same solution can be monitored independently. The ATP sensor A32/Cy5-Rev (K_D = 4.8 μM, Figure S4A) could monitor ATP from a submicromolar to millimolar concentration range at 670 nm (Figure 7C, lane 1). Even when the ATP titration was carried out in the presence of GTP (500 μM), the fluorescence intensity of A32/Cy5-Rev increased (Figure 7C, lane 3) with the affinity similar to that in the absence of GTP (K_D = 7.8 μM, Figure S4C). Increasing the concentration of ATP did not affect the fluorescence intensity of the GTP sensor G33/NBD-Rev (Figure 7C, lane 2). G33/NBD-Rev showed constant fluorescence intensity in solutions containing 500 μM GTP and increasing concentrations of ATP (Figure 7C, lane 4). The GTP sensor G33/NBD-Rev (K_D = 8.6 μM, Figure S4B) also responded to GTP from a submicromolar to millimolar concentration range at 535 nm in the absence (Figure 7C, lane 6) and presence (lane 8) of ATP (500 μM). The affinity

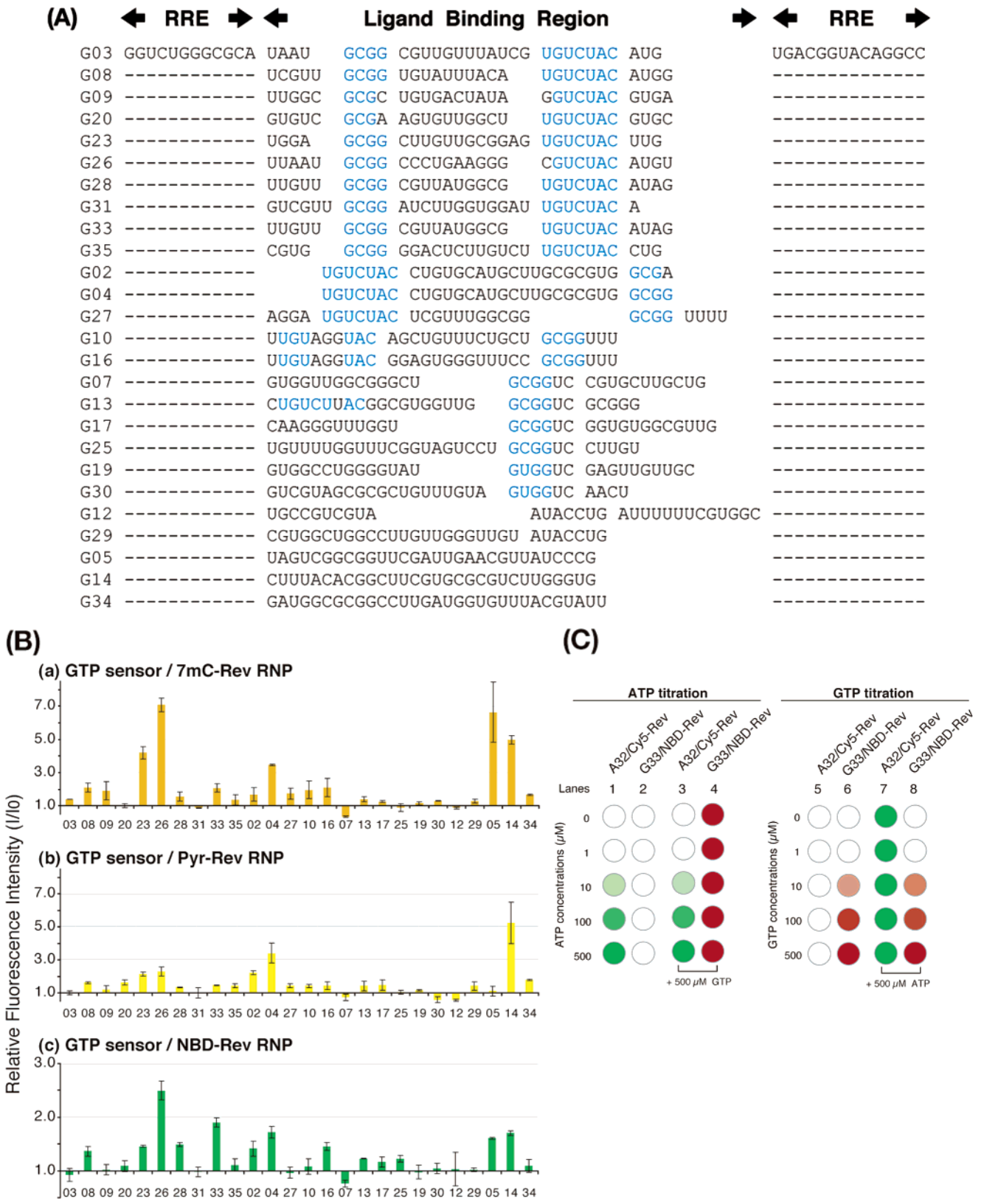

Figure 7. (A) Nucleotide sequences of the N30 ligand-binding region for the RNA subunit of RNP selected against GTP revealed possible consensus nucleotide sequences (shown in blue). RRE denotes the Rev-binding RNA sequence. (B) Relative fluorescence intensities (I/I_0) of fluorescent GTP-binding RNPs upon GTP binding are shown in the bar graphs: (a) 7mC-Rev RNP, (b) Pyr-Rev RNP, (c) NBD-Rev RNP. (C) Titrations of the ATP sensor A32/Cy5-Rev by addition of ATP (1, 10, 100, and 500 μM) showed an increase in the fluorescence intensity both in the absence (lane 1) and in the presence (lane 3) of 500 μM GTP. Fluorescence intensities of the ATP sensor A32/Cy5-Rev were constant upon addition of GTP (1, 10, 100, and 500 μM) in the absence (lane 5) and presence (lane 7) of 500 μM ATP. Fluorescence intensities of the GTP sensor G33/NBD-Rev were constant by addition of ATP (1, 10, 100, and 500 μM) in the absence (lane 2) and presence (lane 4) of GTP (500 μM). Titrations of the GTP sensor G33/NBD-Rev by addition of GTP (1, 10, 100, and 500 μM) showed an increase in the fluorescence intensity both in the absence (lane 6) and in the presence (lane 8) of 500 μM ATP. Fluorescence intensities were monitored at 670 and 535 nm for A32/Cy5-Rev and G33/NBD-Rev, respectively.

of the GTP sensor G33/NBD-Rev to GTP in the presence of 500 μM ATP (K_D = 9.7 μM, Figure S4D) was almost equal to that in the absence of ATP (K_D = 8.6 μM, Figure S4B).

Conclusions

The combinatorial strategy using the modular RNP receptor reported here enables efficient tailoring of fluorescent sensors for specific ligands, ATP and GTP. The approach consisting of a selection followed by a screen, in vitro selection of RNP receptors and a convenient screening of the combinatorial RNP sensor library, affords fluorescent biosensors with a variety of emission wavelengths, high I/I_0 ratios, and/or responding ligand concentration ranges without a chemical modification of the ligand-binding RNA region and without detailed knowledge of the three-dimensional structure for the RNP receptors. By choosing the fluorescent RNP sensors with appropriate optical properties, sensitive detections of multiple ligands without inhibitory effects of intrinsic fluorescence in the samples such as cellular extracts would be possible.

Combination of the fluorescent RNP sensors offers a fluorescent sensing system that covers a wide range of ligand concentrations. Fluorescent sensor systems with wide detection concentration ranges were previously achieved[6−10] by manipulating the ligand-binding affinity of the parent receptor by means of site-directed mutations that required detailed knowledge of three-dimensional structural information. In contrast, in vitro selection of the RNA-based RNP library automatically provides RNP receptors with various affinity to the target ligands. Such an inherent diversity of the ligand-binding affinity is a definitive advantage for RNP to build a fluorescent sensor.

We have previously reported that in vitro selection from the RNA-based RNP library followed by a selection from the peptide-based RNP library affords an ATP-binding RNP with higher affinity to ATP and a distinct specificity for ATP versus dATP than the ATP-binding RNP receptor obtained by in vitro selection from the RNA-based RNP library.[32] Such RNP receptors with enhanced affinity and selectivity to the ligand would allow tailoring RNP sensors with higher selectivity to the target ligands. The noncovalent modular structure of RNP provides a distinct advantage for the screening strategy of fluorescent sensors described here. Once an optimal fluorescent RNP sensor is obtained, the noncovalent complex of RNP sensor could be covalently linked by tethering between the RNA and the fluorophore-labeled peptide subunits, which is currently underway. Such a stable RNP sensor can be immobilized by hybridization of the attached RNA sequences to complementary surface-bound DNA probes[34,35] to organize an RNP sensor microarray that is quite useful for analyzing biologically active molecules simultaneously.

Materials and Methods

Materials. ATP-agarose (immobilized on cross-linked 4% beaded agarose), GTP-agarose (immobilized on cross-linked 4% beaded agarose), and nucleotides (ATP, UTP, CTP, and GTP) were purchased from Sigma-Aldrich. Fmoc-protected amino acids and HATU were from Nova Biochem and Applied Biosystems, respectively. Fluorophores, 4-fluoro-7-nitrobenz-2-oxa-1,3-diazole (NBD fluoride), 1-pyrenesulfonyl chloride, and 7-methoxycoumarin-3-carboxylic acid, were from Molecular Probes. Cy5 mono NHS ester was from Amersham Biosciences.

Synthesis of Oligopeptides and Fluorophore Coupling Reactions. Peptides were synthesized on a Shimadzu PSSM-8 peptide synthesizer according to the Fmoc chemistry protocols by using Fmoc-PAL-PEG resin (0.41 mmol/g, Applied Biosystems), protected Fmoc-amino acids, and HATU. Fluorophore with activated group was directly coupled to N-terminal deprotected Rev peptide on the resin in DMF containing 5% (v/v) DIEA. 7-Methoxycoumarin-3-carboxylic acid was reacted with N-terminal deprotected peptide-resin in DMF containing 5% (v/v) DIEA, HATU. The labeled peptides were then deprotected and cleaved from the resin, gel filtrated with G-10 resin, purified by a reversed phase HPLC, and characterized by Voyager MALDI TOF spectrometry (Applied Biosystems). Peptide concentrations were determined using amino acid analysis.

Nucleic Acids Preparations. The original double-stranded DNA pools were constructed by Klenow polymerase (New England Biolabs) reaction from a synthesized oligonucleotide containing 30 random nucleotides (5-GGAATAGGTCTGGGCGCA-(N30)-TGACGGTA-CAGGCCGAAAG-3′) and a 3′-DNA primer (5′-CTTTCGGCCTG-TACCGTCA-3′), followed by PCR amplification to add the promoter for T7 RNA polymerase using Pyrobest DNA polymerase (TaKaRa) with the 3′-DNA and a 5′-DNA primer (5′-TCTAATACGACTCAC-TATAGGAATAGGTCTGGGCGCA-3′: T7 RNA promoter is underlined). RNA transcription was performed using AmpliScribe T7 Kit (Epicentre) for 3 h at 37 °C according to a supplier's recommended protocols. The resulting RNA was phenol/chloroform extracted, precipitated with ethanol, and pelleted by centrifugation. The RNA was purified by denaturing polyacrylamide gel electrophoresis and eluted. Concentrations of RNAs were determined by UV spectroscopy.

Preparation of Ribonucleopeptide Receptor. Ribonucleopeptide complexes that bound ATP or GTP were selected as follows: RNA was heated at 80 °C for 3 min and cooled to room temperature for 2 h for proper secondary structure. A binding buffer (100 μL, 10 mM Tris-HCl (pH 7.6), 100 mM NaCl, 10 mM $MgCl_2$) containing 1 μM RNA, 1.5 μM Rev, and a 50 μL volume of ligand-conjugated agarose was incubated to allow a formation of a specific ribonucleopeptide complex for 30 min on ice. RNA−peptide−resin complexes were washed three times with 300 μL (6-volume of resin) of binding buffer to remove unbound RNA−peptide complexes and eluted three times with 150 μL (3-volume of resin) of binding buffer containing 4 mM of cognate ligands. Recovered ribonucleopeptide complexes were precipitated with ethanol and resuspended in TE buffer. After reverse transcription with AMV reverse transcriptase (Promega) of the selected RNA using the 3′-DNA primer used in PCR amplification and successive PCR amplification (RT-PCR) using the 5′- and 3′-DNA primer, DNA templates were transcribed, and the resulting RNAs were subjected to the next round of selection. Selected RNA pools were converted to DNA and PCR-amplified to introduce *Bam*HI, *Eco*RI restriction sites by using primers 5′-GCGGGATCCTTTCGGCCTG-TACCGTCA-3′ and 5′-CGGAATTCTAATACGACTCACTATAGG-3′. After enzymatic digestion (New England Biolabs), DNAs were cloned into the pUC19 vector using Ligation Kit Version 2 (TaKaRa) and sequenced using a BigDyeTerminator Cycle Sequencing Kit (Applied Biosystems) with a model 377 DNA sequencer (Applied Biosystems).

Competition Binding Assays. The competition assays were performed as follows. A binding buffer (40 μL) containing 10 mM Tris-HCl (pH 7.6), 100 mM NaCl, 10 mM $MgCl_2$, 0.005% Tween20, 1 μM ^{32}P-labeled RNA, 1 μM Rev peptide, and a 20 μL volume of ATP-agarose was incubated for 30 min at ambient temperature in the presence of competitive ligand. Ribonucleopeptide−ATP complexes were washed with 200 μL of binding buffer to remove unbound ribonucleopeptides and eluted three times with 100 μL of binding buffer containing 5 mM ATP. The fractions of RNA bound to the ATP resin were

(34) Weng, S.; Gu, K.; Hammond, P. W.; Lohse, P.; Rise, C.; Wagner, R. W.; Wright, M. C.; Kuimelis, R. G. *Proteomics* **2002**, *2*, 48−57.
(35) Collett, J. R.; Cho, E. J.; Ellington, A. D. *Methods* **2005**, *37*, 4−15.

quantitated by Cherenkov counting in a scintillation counter (Beckman multi-purpose scintillation counter LS6500).

Fluorescence Spectral Measurements. Fluorescence spectra were recorded on a Hitachi F-4500 fluorescence spectrofluorophotometer with excitation and emission bandwidth of 5 nm at 20 °C. All measurements were performed in a buffer (300 μL) containing 10 mM Tris-HCl (pH 7.6), 100 mM NaCl, 10 mM $MgCl_2$, fluorescent RNP (0.5 μM or 0.1 μM), and the indicated concentration of ligand. Excitation wavelengths were Pyr-Rev (357 nm), 7mC-Rev (360 nm), and 7mC-GRev (360 nm).

Fluorescence Measurements on the Microplate. The 96-well fluorescence measurements were performed on a Wallac ARVOsx 1420 multilabel counter. A binding solution (100 μL) containing 1 μM of fluorescent RNP in 10 mM Tris-HCl (pH 7.6), 100 mM NaCl, 10 mM $MgCl_2$ with indicated concentration of ligand was gently swirled for a few minutes and allowed to sit for 30 min at 20 °C. Emission spectra were measured with an appropriate filter set for each fluorophore. Excitation and emission wavelengths were Pyr-Rev (355, 390 nm), 7mC-Rev (355, 390 nm), NBD-Rev (475, 535 nm), and Cy5-Rev (650, 670 nm). Images of the fluorescence intensity of wells were obtained by using the Wallac 1420 software version 2.00. Color-coded images of fluorescent intensity of each well were obtained by using the Wallac 1420 software version 2.00.

Determination of Binding Affinity. The ATP-binding affinity of fluorescent RNP was obtained by fitting the ATP titration data using the equation:

$$F_{obs} = A(([FRNP]_T + [ATP]_T + K_D) - (([FRNP]_T + [ATP]_T + K_D)^2 - 4[FRNP]_T[ATP]_T)^{1/2})/2[FRNP]_T$$

where A is the increase in fluorescence at saturating ATP concentrations ($F_{max} - F_{min}$), K_D is the dissociation constant, and $[FRNP]_T$ and $[ATP]_T$ are the total concentrations of fluorescent RNP and ATP, respectively. The GTP-binding affinity of fluorescent RNP was obtained similarly.

Acknowledgment. This work was supported in part by the Grants-in-Aid for Scientific Research from the Ministry of Education, Science, Sports, and Culture, Japan, to T.M. (No. 17310125 and No. 17026019).

Supporting Information Available: Results of ATP-binding titration assay of the A28/Rev RNP complex (Figure S1), relative fluorescence intensity changes (I/I_0) of 7mC-GRev RNPs upon ATP binding (Figure S2), selectivity of ATP and GTP sensors (Figure S3), and fluorescence titration assay of ATP sensor A32/Cy5-Rev and GTP sensor G33/NBD-Rev (Figure S4). This material is available free of charge via the Internet at http://pubs.asc.org.

JA063965C